VARIATIONS OF SOLAR RADIUS: OBSERVATIONS WITH RHESSI

M. D. Fivian, H. S. Hudson, and R. P. Lin

Space Sciences Laboratory, University of California

ABSTRACT

The Solar Aspect System (SAS) of the rotating (15 rpm) RHESSI spacecraft has three subsystems. Each of these measures the position of the limb by sampling the solar chord profile with a linear CCD and a narrow-bandwidth filter at 670 nm. With a plate scale of 1.7 arcsec/pixel, the precision of each of the six simultaneously observed limb positions is observed to be better than 50 mas, using four pixels at each limb. Since the launch of RHESSI early 2002, solar limbs have been measured at about 100 samples/sec. This has provided a database of 7×10^9 single radius measurements at the time of writing. The main function of SAS is to determine the RHESSI pointing relative to Sun center. Using these data we find that we can readily measure the solar oblateness at a magnitude consistent with other recent measurements. We can also see clear signatures of sunspots and faculae near the limb.

Key words: Sun, solar radius, solar limb.

1. INTRODUCTION

The RHESSI[1] spacecraft observes solar hard X-rays and γ-rays via rotational image modulation. From the reference frame of the rotating spacecraft, the Sun appears to move in circles, nominally of a few arc min amplitude, and these circles themselves move semi-regularly in "coning" motions whose amplitudes depend on varying external torques. In order to achive sub-arcsecond imaging in spite of these complex motions, the RHESSI attitude sensors (Fivian et al. 2002; Hurford & Curtis 2002) must have the ability to provide aspect information instantaneously at the desired accuracy. This requirement then dictated frequent measurements of the solar limb location (spacecraft X and Y coordinates) by the Solar Aspect Sensor (SAS).

In this paper we briefly describe SAS (for full details, see Fivian et al., 2002) and its data. We then show that these data provide interesting measurements of the solar limb, which we plan to use to observe the shape of the Sun and to monitor its variability. Since these are among the first "solar oblateness" observations from space, we hope that they will have superior quality to previous ground-based and balloon-borne observations. As an additional byproduct SAS provides detailed observations of solar activity (sunspots and faculae) as they traverse the limb. It is not clear that there are meaningful applications of these data, but since their perspective is so different from the usual observations, we speculate about this possibility.

2. OBSERVATIONS

SAS consists of three simple telescopes, with lenses mounted on the front grid tray and linear CCD sensors on the rear grid tray (1). The CCDs have 2048 pixels subtending 1.7 arcsec/pixel through narrowband filters at 670 nm. Each sensor makes an image of a chord across the solar disk, as illustrated in Figure 2. The basic data-reduction procedure uses the limb-crossing data (six items under typical pointing conditions, but fewer if the RHESSI pointing is not good) to define Sun center. The measure of precision in this calculation is the size of the "error triangle" reflecting the degree of disagreement among the sensors. The problem is overdetermined if six limbs are available. The individual limb crossing then can
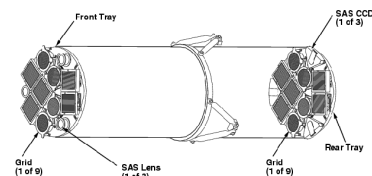

Figure 1. Sketch of RHESSI. The X-ray/γ-ray imager points to the left, and the two sets of grids form nine rotating modulation collimators. The SAS instrument essentially of three lenses on the front grid tray and three linear CCDs on the rear grid tray.
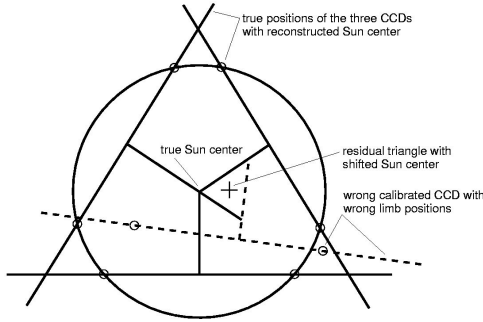
---

[1]The Reuven Ramaty High-Energy Solar Spectroscopic Imager; see Lin et al. (2002).

Figure 2. Functional layout of SAS images, showing the "error triangle" used to estimate the systematic errors between the subsystems.
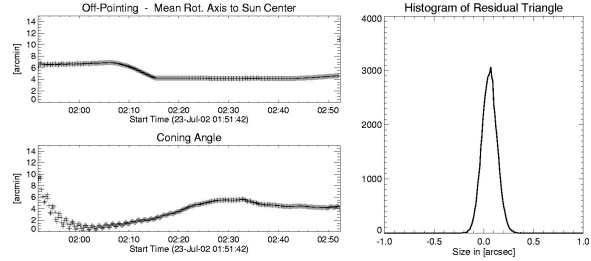

Figure 3. Typical orbital variation of RHESSI pointing and coning, together with the resultant error triangle distribution. Note that the width of this distribution is well below one arc sec, as required for the primary function of RHESSI to provide Sun-center location for X-ray and γ-ray imaging.

be interpreted directly as a radius, based upon the known sensor geometry and the derived Sun center position; finally this radius point can be assigned to a specific position angle around the limb by use of the independent information from the roll aspect sensors on board RHESSI (Fivian et al. 2002; Hurford & Curtis 2002).

The SAS data include full chords, telemetered several times per 96-minute orbit for each sensor, and routine limb data. The routine data consist of a programmable set of pixels, nominally four, around the position of the crossing point of a present threshold. The frequency of these data is again programmable, but for the first three years of RHESSI operation it was usually set at 16 samples each second, thus 96 individual limb readings (two each for each of three sensors) or about 400 limb points per RHESSI rotation (nominally 4 sec period). The limb data in general convolve geometry and brightness and in the basic reduction, as well as the preliminary data analysis described below, we have used fits of four pixels at the limb to an average apparent limb profile function.

We derive flat-field corrections by use of the full scans, assuming the quiet-Sun signal to remain constant on the average. In work to date this flatfielding has involved a simple algorithm for rejecting outlier points, such as those from sunspots. The principal noise in individual scans appears to come from solar convection and p-modes, at the level of a few percent rms. The flatfield data derived in this manner are stable and reproducible to a few parts per million; we speculate that future more precise analysis may require the re-generation of flatfield data via the use of masks based on Ca (or other) chromospheric images; this would allow us to reject systematic errors due to plage and enhanced network. Figure 3 shows results for the error-triangle distribution in a representative RHESSI orbit.

The data reduction to date has been carried out using the tools developed for Sun-center determination in support of the RHESSI primary observations. This "zeroth order" data reduction does not include refinements such as dark correction, flatfielding, or corrections for systematic errors. We show the effect of some of these in Figures 4 and 5 in the form of raw limb position vs time for a rep-
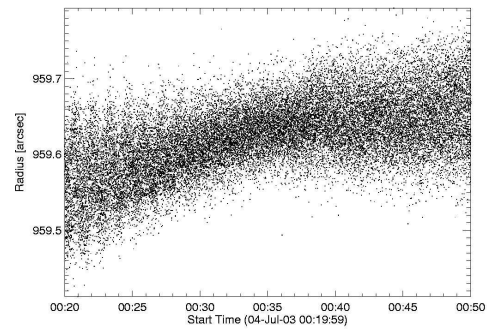

Figure 4. Typical sample of data from one limb cut from one sensor. This illustrates the abundance of data and also reveals some of the systematic errors. The oscillation seen early in the time series result from the coning motion of the spacecraft, with apparent limb variation due to small calibration errors. The general rise probably reflects an uncompensated temperature dependence.

resentative segment of the data. We expect that making these corrections and adjustments to the raw data will result in much-improved errors. We expect that the triple redundancy of the data along with the rotation, which makes differential measurement much easier, will provide significant reductions of the systematic errors seen in the zeroth-order data reduction.

3. DATA ANALYSIS

3.1. Spots and faculae

Given the preliminary nature of the data reduction, we do not present any quantitative analysis in this paper. We illustrate some features of the data instead, demonstrating (we hope) that quantitative analysis will soon be possible.

An overall view of the data can be obtained from gray-scale stackplots of limb location vs. position angle and
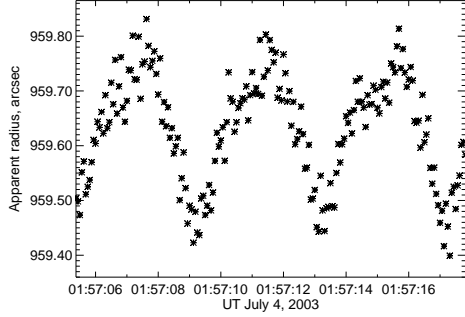
Figure 5. *Expanded view of data similar to the Figure 4. One can now see the limiting random error in the data, which amounts to about 30 mas (10^{-3} arc sec, roughly parts per million). The cyclical variation of about 300 mas results from coning motions of the RHESSI rotation and can easily be removed.*
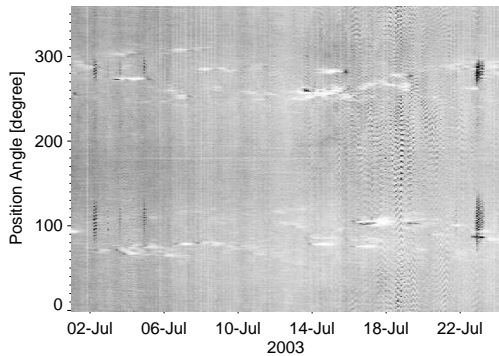

Figure 6. *Stackplot displaying apparent solar radius (grayscale) vs limb position angle and time. The compact dark features are spots transiting the limb, and the white features faculae. The vertical streaking at the right side of the figure shows the growth of systematic errors due to subtle time variations of the calibration parameters, which this zeroth-order data data reduction has not corrected.*

time. Figure 6 shows a first example of this. There are many signs of faculae (dark patches) at the active latitude zones around PA 90° and 270°, near the equator. Such signatures result in systematic radius errors and need to be removed for analysis of the mean solar figure.

An enlarged view of one region of Figure 6 appears in Figure 7, with the PA and time scales adjusted so that the sunspots appear almost round in this pseudo-image. The passage of a large sunspot across the limb makes the radius appear locally smaller. The radius should in fact be physically smaller because of the Wilson depression (e.g., Solanki 2003). Unfortunately we do not know yet how much of the apparent limb signal shown in Figure 7 to ascribe to this effect, and how much to ascribe to the darkness of the spot itself. A future analysis based upon an improved limb definition and modeling should allow us to measure the true Wilson depression. It is interesting
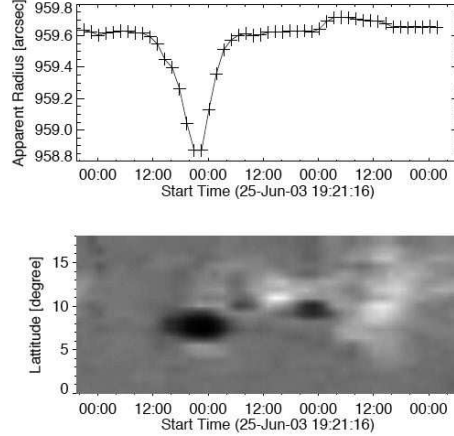

Figure 7. *Pseudo-image made from the stackplot (lower panel) of a small region at the limb, showing the E limb passage of NOAA AR397 (June 25, 2003). The plot (upper) shows radius values along the line at 6° latitude. Note that the dip is not exactly the Wilson depression, but rather a convolution of limb position and brightness in the spot. The facular brightness excesses similarly appear as larger radii and are also uncalibrated in terms of radius vs. brightness contribution.*

in this context to note that (Solanki 2003) cites a Wilson depression of 700 km, a substantial fraction of what we see in Figure 7.

In general the limb presents a difficult problem for precise local definition because of the complicated dynamics there. The local limb-darkening function will vary with time depending upon convective flows and upon the p-mode oscillations, among other things. Probably the best quantitative approach would be to relate the RHESSI limb observations to hydrodynamic (or MHD) simulations of the flows (Carlsson et al. 2004; Steiner 2005).

3.2. Oblateness

As is well known, the rotation of the Sun induces a deformation of its figure, and we can characterize the lowest-order harmonic of this deformation as an oblateness signal. Rozelot et al. (2003) discuss the recent history of such measurements, as summarized in Figure 8. The best recent measurements (Kuhn et al. 1998; Rozelot et al. 2003) are consistent with the oblateness inferred from the solar surface rotation. The best observations have uncertainties on the order of 1 mas, roughly 10% of the observed oblateness value. This can be compared with the preliminary look at the RHESSI data given in Figure 9. There is no quantitative result yet in this Figure, but roughly speaking the oblateness is of the right order of magnitude. Note that this plot represents a large amount of data, far more than should be necessary based upon the observed magnitude of the random error. The point-to-point variation seen in Figure 5, which amounts
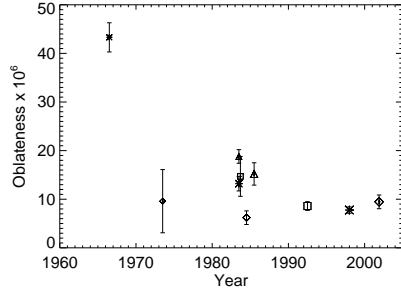
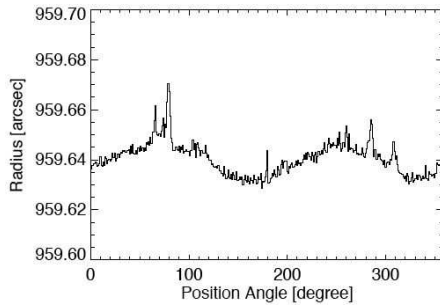*Figure 8. Recent history of solar oblateness measurements.*

Figure 9. Summation of about three days' data from the stackplot of Figure 6. This shows a clear oblateness signal at about the right amplitude, together with many excess peaks due to faculae at the limb.

to about 30 mas, suggests that a 10σ result on oblateness should be achieved with 10 s of data, rather than three days' worth!

We anticipate that further work with these data will make it possible to determine the oblateness to an error level considerably better than that of the existing measurements. If this becomes possible then we should also be able to measure or set interesting limits on higher-order terms in the harmonic expansion of the limb shape.

4. CONCLUSIONS

The data from the RHESSI limb sensors enable studies of the shape of the solar limb and its time variation. We have shown that the sampling and precision of these observations is sufficient for studies of the solar oblateness, and probably higher-order shape components as well.

The data also abundantly show the effects of solar magnetic activity in the form of sunspots and faculae. We hope to be able to do useful things with these data, such as to track the cyclic motions of the polar faculae (e.g., Sheeley 1991). We would also like to be able to study limb flares in detail, including white-light prominences (e.g., Leibacher et al. 2004) as well as more classical white-light flare emission from flare footpoints. There is

little information in the recent literature about the limb-darkening function of white-light flare emission.

As a speculation, we consider the effect of the large-scale coronal magnetic field on the solar radius. The ratio of gas pressures in the corona and at the limb (the upper photosphere) should be of the order of parts per million, within the range of the RHESSI shape determination. Since the mean coronal pressure may vary by a factor of ten between the closed and open corona, it may be possible to detect limb signatures of coronal holes.

The time variability of the solar radius as a basic astronomical parameter, $R_\odot$, has become especially interesting since changes in the total irradiance were first clearly recorded (Willson et al. 1981). This kind of measurement challenges the observer to get complete control of systematic errors in the measurement, an almost impossible task. Thus in the field of total irradiance it is recognized that overlapping data sets can help in the characterization of long-term changes. We suggest that the same logic applies here, and that the RHESSI observations of solar radius should overlap those of the PICARD project (Thuillier et al. 2003) if at all possible.

REFERENCES

Carlsson, M., Stein, R. F., Nordlund, Å., & Scharmer, G. B. 2004, *ApJL*, 610, L137

Fivian, M., Hemmeck, R., Mchedlishvili, A., & Zehnder, A. 2002, *Solar Phys*, 210, 87

Hurford, G. J. & Curtis, D. W. 2002, *Solar Phys*, 210, 101

Kuhn, J. R., Bush, R. I., Scherrer, P., & Scheick, X. 1998, *Nature*, 392, 155

Leibacher, J. W., Harvey, J. W., Kopp, G., Hudson, H., & GONG Team. 2004, American Astronomical Society Meeting Abstracts, 204,

Lin, R. P., Dennis, B. R., Hurford, G. J., et al. 2002, *Solar Phys*, 210, 3

Rozelot, J., Lefebvre, S., & Desnoux, V. 2003, *Solar Phys*, 217, 39

Sheeley, N. R. 1991, *ApJ*, 374, 386

Solanki, S. K. 2003, *Astron. Astrophys. Revs.*, 11, 153

Steiner, O. 2005, *Astron. Astrophys.*, 430, 691

Thuillier, G., Joukoff, A., & Schmutz, W. 2003, in ESA SP-535: Solar Variability as an Input to the Earth's Environment, 251–257

Willson, R. C., Gulkis, S., Janssen, M., Hudson, H. S., & Chapman, G. A. 1981, Science, 211, 700